Received: 21 February 2023 | Revised: 25 April 2023 | Accepted: 21 May 2023

IET Energy Systems Integration

DOI: 10.1049/esi2.12105

ORIGINAL RESEARCH

Decoupling and dimension reduction method for distribution system security region

Jun Xiao[1] | Yuhao Fan[1] | Xun Jiang[2]

[1]Key Laboratory of Smart Grid of Ministry of Education, Tianjin University, Tianjin, China

[2]School of Engineering, Cardiff University, Cardiff, UK

Correspondence

Xun Jiang, School of Engineering, Cardiff University, Cardiff, UK.
Email: jiangx28@cardiff.ac.uk

Funding information

National Natural Science Foundation of China, Grant/Award Number: 52177105

Abstract

The application of the security region methodology in a practical distribution system with large scale normally requires large computer memory and high computation time. To overcome this problem, this article proposes a decoupling and dimension reduction method, which can significantly accelerate the calculation of distribution system security region (DSSR) and is important for the application of the DSSR theory in large-scale distribution systems. First, the definition of DSSR dimension reflecting the size of solution space and the time complexity is proposed. And the solution algorithm for DSSR dimension is also given. Second, a decoupling and dimension reduction method suitable for the analysis of DSSR is proposed. Following the method, an incidence matrix can be obtained from the DSSR expressions, which can be further divided into multiple block matrices. According to the feeder combinations of the block matrices, the distribution system can be decoupled into multiple sub-networks for more efficient analysis. Finally, a 10kV distribution network is used in case study to validate the proposed method. The results for a time-consuming calculation, that is, TSC curve calculation, show that the proposed method can reduce the computation time significantly, making the time-consuming calculation suitable for the analysis of large-scale cases.

KEYWORDS

decoupling, dimension reduction, distribution system, incidence matrix, security region

1 | INTRODUCTION

The concept of security region originates from transmission system. Since the static security region of transmission system was proposed in 1975 [1], a series of relatively complete theories of transmission system security region have been established [2–5]. Some scholars have introduced the concept of security region into distribution system and proposed distribution system security region (DSSR). DSSR [6] is defined as a set of operating points that satisfy the distribution system N-1 secure. Furthermore, the model, topological characteristics [7], simulation observation [8], and mathematical deduction [9] of DSSR are also analysed.

Since the 'region' method has convincing advantages over the 'point-wise' method, some scholars use DSSR to develop new analysis methods about distribution system. The static voltage region of distribution system is proposed in ref. [10] to solve the deficiency of simplifying the reactive power part in original operation area. Based on 'region' method, the maximum uncertainty of active distribution system is described by the upper bound of operating points satisfying voltage and current constraints [11]. The trend characteristics of power systems can be obtained through situation awareness methods [12, 13]. The minimum variance coefficient of security distance is taken as an objective function in the new network reconfiguration model to show that the model can satisfy N-1 security [14]. In addition, boundary supply capability (BSC) [15] and security distance [16] for distribution systems are proposed based on DSSR. The concept and method of DSSR have also been extended to areas such as integrated energy systems [17, 18].

The scale of a power system depends on transforming capacity, the number of substations, line-length and the

number of loops and so on [19]. Evaluation indicators and analysis methods are proposed to reflect the sufficiency level of the scale of networks [20]. For distribution system, a complete evaluation indicator system and comprehensive model of distribution network scale are established based on the principle of grey relational analysis and analytic hierarchy process [21]. The scale of DSSR is also a fundamental issue in the study of the DSSR.

The scale of an object or system can be described as dimension [22]. Dimension can be represented by the number of parameters required to describe an object [23]. Two forms of DSSR dimension are proposed to describe the scale of DSSR [24]. One is named binary dimension: it is defined with two variables, the number of security boundaries (Q_b) and the number of variables (Q_v) in them. The other is named unary dimension: the number of equivalent feeders is introduced, denoted as N_e, and the DSSR dimension is donated as D_u, which is expressed in the most commonly used form of $N_e \times N_e$.

The research of the DSSR dimension has a certain foundation, but the large scale of the real distribution system leads to a very high dimension of its security region. To address this challenge, dimension reduction methods for DSSR are required. Existing dimension reduction methods in DSSR research are primarily employed for visualising DSSR. In these methods, the power injections at two or three important nodes in the distribution system are selected for visualisation while keeping the power injections at other nodes constant. The authors in refs. [10, 25], and [26] visualised the static security region of the distribution network in 2-dimensional cross sections. Wan et al. [11] study the high-dimensional boundary by mapping the maximum uncertainty boundary of distributed generators in active distribution networks to a 2-dimensional plane. Effective decoupling methods for DSSR have not been proposed in existing studies. Therefore, this paper proposes a decoupling and dimension reduction method for DSSR. The superiority of the proposed method is in the dimension reduction of the expression of DSSR, which can significantly improve the calculation speed of DSSR-associated calculations. The main contributions of this paper include:

(1) A more effective definition of DSSR dimension comparing to the existing relevant study is proposed for dimension reduction of DSSR, which can further contribute to the decoupling of distribution systems.
(2) A DSSR dimension calculation method based on DSSR expressions and incidence matrix is proposed, which has demonstrated its effectiveness in reducing the dimension of DSSR.
(3) A decoupling and dimension reduction method for DSSR is proposed to enable rapid security region-based analysis and accelerate the security analysis of the real-world distribution systems. The effectiveness of the proposed method has been validated by calculating Total Supply Capability (TSC) curve. Compared to the existing method for calculating TSC curve, the proposed method can significantly increase the calculation speed while reducing the memory requirement.

2 | DSSR DIMENSION

2.1 | Background of DSSR dimension

The cardinality of a finite set represents the size of the set, which is just the number of elements in the set. And if a vector space V has a basis of cardinality K, we say that V is K-dimensional [23]. Similarly, the DSSR dimension describes the size of DSSR space. Higher dimension requires more parameters to describe a DSSR, which indicates that the DSSR problem has a larger scale.

Two forms of DSSR dimension are proposed to describe the scale of DSSR [24]. One is defined with two parameters, the number of security boundaries and the number of variables in them. Although this definition can represent the scale of the security region, there are shortcomings: firstly, the two-parameter approach is not normal for DSSR users to construct the problem space; secondly, comparing the scale of two DSSRs is difficult when the comparison results of these two parameters are not consistent. Thus, another form of DSSR dimension is defined with one parameter, that is, the number of equivalent feeders, which is denoted as N_e. For the distribution network with N feeders, after considering the feeder link, it is equivalent to the full contact distribution system with N_e feeders, and the dimension is $N_e \times N_e$. This dimension cannot completely distinguish feeders with links. For example, the real dimension of a distribution network with n single-links is 2, but the result of unary dimension is $\frac{4n}{\sqrt{9n-5}} \times \frac{4n}{\sqrt{9n-5}}$ [24]. In ref. [24], the researchers clarify that a distribution network with n single-links is equivalent to a virtual full-link network with $\frac{4n}{\sqrt{9n-5}}$ feeders. The unary dimension is the square of the number of the feeders in the equivalent full-link network. The details on how to obtain the number of the feeders of equivalent virtual full-link network can refer to [24]. The definition of DSSR dimension in ref. [24] is not convenient to use since it is computationally complex and hard to be obtained from the incidence matrix of the DSSR expressions.

2.2 | A new definition of DSSR dimension

In order to overcome the shortcomings of large computational cost and difficult transformation of incidence matrix and to conform to the traditional definition of dimension as well, an integer responding to the number of parameters, a new DSSR dimension is defined in this paper. The number of parameters is the number of linked feeders, the maximum of which determines the dimension of DSSR space.

For a distribution network with N feeders, the DSSR dimension D_m is denoted as

$$D_m = \max\{m_1, m_2, ..., m_i, ..., m_k\} \quad (1)$$

k is the number of groups of feeder combinations. A feeder combination is the combination of feeders linked with each other through the tie switches [24]. m_i is the number of feeders in the ith feeder combination. Physically, the DSSR dimension D_m in this paper denotes the maximum number of feeders which link with each other in a distribution system. This dimension partly reflects the interdependence of the feeders in the distribution system, which can be used for decoupling the distribution system.

2.3 | Relationship between DSSR dimension and time complexity of DSSR calculation algorithms

Assuming that n is the size or number of input data, $T(n)$ is the execution times of a given code. Algorithms generally use a simplified estimate O($f(n)$) of $T(n)$ to measure the execution speed of the code, and this simplified estimate O($f(n)$) is called the time complexity [27]. The time complexity O($f(n)$) is the extent to which the solution time increases when the input variable n increases.

The DSSR dimension expresses the scale of DSSR problem, thus determining the complexity of constructing DSSR or searching optimal solutions in DSSR space by using a specified algorithm. The DSSR dimension and the time complexity of DSSR calculation algorithms have one-to-one correspondence. For example, for the calculation of TSC curve [28], if the dimension of the power grid is D_m, then the time complexity of the conventional TSC curve algorithm is O(n^{Dm}).

3 | DSSR DIMENSION CALCULATION METHOD

The steps of the method for calculating the DSSR dimension are as follows. For clarity, each step is explained with a five-feeder case network as shown Figure 1.

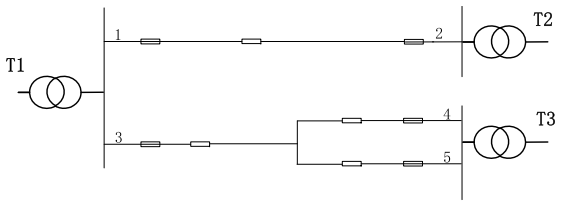

FIGURE 1 A five-feeder case network for illustrating the calculation steps of distribution system security region (DSSR) dimension.

3.1 | DSSR expression

Step 1: Obtain the DSSR expression $\mathbf{\Omega}_{\mathrm{DSSR}}$ based on detailed feeder interconnection relationship and component parameters (including the transformer and feeder capacities) of the distribution system [7]. DSSR is defined as the set of all operating points that satisfy N-1 security constraints of the distribution system. Therefore, the feeder load and transformer load should satisfy N-1 security constraints including feeder N-1 security constraints and transformer N-1 security constraints.

1-1: Feeder N-1 security constraints indicate that the power load at the feeder out of service can be transferred to other connected feeders through tie switches, which do not incur any overloading problem. Assuming feeder m is out of operation after N-1 contingency, the power load at feeder m can be transferred to feeder n via the tie switch, then the N-1 constraint for feeder m can be expressed as follows:

$$S_{F,m} + S_{F,n} \le c_{F,n}(\forall m, n) \quad (2)$$

where $S_{F,x}$ ($x = m, n$) is the power load supplied by feeder x; $c_{F,n}$ is the capacity of feeder n. Equation (2) guarantees that after load transfer from feeder m to feeder n, no overload problems occur. N-1 security constraints for other feeders can follow the same principle as in Equation (2).

Take the N-1 security constraint for feeder 1 of the case in Figure 1 as an example, when feeder 1 is out of operation after N-1 contingency, the power loads $S_{F,1}$ at feeder 1 can be transferred to feeder 2 via the tie switch. Then the N-1 constraint for feeder 1 can be expressed as follows:

$$S_{F,1} + S_{F,2} \le c_{F,2} \quad (3)$$

In Figure 1, there is also a two-supply-one-backup connection mode containing feeder F3, F4, F5. For brevity, feeder F3 is used as a backup for feeder F4 and F5.

1-2: Transformer N-1 security constraints express the security after N-1 contingency at each transformer, in a similar way as feeder N-1 security constraints. When transformer i is out of operation after N-1 contingency, all its feeder loads are transferred to other transformers via the tie switches. The security constraint regarding transformer i should guarantee that no overloading problems occur in all the transformers after N-1 contingency at transformer i, which is expressed in Equation (4),

$$S_{T,tr}^{i,j} + S_{T,j} \le c_{T,j}(\forall i, j) \quad (4)$$

where $S_{T,tr}^{i,j}$ is the load transferred from transformer i to transformer j; $c_{T,j}$ is the rated capacity of transformer i.

Take the N-1 constraint for transformer T_1 of the case in Figure 1 as an example, when transformer T_1 is out of

operation after N-1 contingency, its power load $S_{F,1}$ at feeder F1 should be transferred to transformer 2 via the tie switch, and the power load $S_{F,3}$ at feeder F3 should be transferred to transformer T_3. The N-1 constraint for transformer T_1 can be expressed as follows:

$$\begin{cases} S_{F,1} + S_{F,2} \le c_{T,2} \\ S_{F,3} + S_{F,4} + S_{F,5} \le c_{T,3} \end{cases} \tag{5}$$

In summary, the DSSR expression $\mathbf{\Omega}_{\mathrm{DSSR}}$ consisting of the above constraints can be formulated as

$$\mathbf{\Omega}_{\mathrm{DSSR}} = \left\{ W \middle| \begin{matrix} S_{F,m} + S_{F,n} \le c_{F,n} (\forall m, n) \\ S_{T,tr}^{i,j} + S_{T,j} \le c_{T,j} (\forall i, j) \end{matrix} \right\} \tag{6}$$

For the case in Figure 1, the DSSR expression $\mathbf{\Omega}_{\mathrm{DSSR}}$ can be formulated as

$$\mathbf{\Omega}_{\mathrm{DSSR}} = \left\{ W \middle| \begin{matrix} S_{F,1} + S_{F,2} \le c_{F,2} \\ S_{F,2} + S_{F,1} \le c_{F,1} \\ S_{F,3} + S_{F,4} \le c_{F,4} \\ S_{F,4} + S_{F,3} \le c_{F,3} \\ S_{F,5} + S_{F,3} \le c_{F,3} \\ S_{F,1} + S_{F,2} \le c_{T,2} \\ S_{F,3} + S_{F,4} + S_{F,5} \le c_{T,3} \\ S_{F,2} + S_{F,1} + S_{F,3} \le c_{T,1} \\ S_{F,4} + S_{F,5} + S_{F,1} + S_{F,3} \le c_{T,1} \end{matrix} \right\} \tag{7}$$

3.2 | Incidence matrix

Step 2: Generate the incidence matrix from the DSSR expression.

The incidence matrix [24] is used to store the linking relationship between feeders in a distribution system, which is denoted as $\boldsymbol{A}$ as follows:

$$A = [a_{ij}] \tag{8}$$

where a_{ij} is the link between feeder i and feeder j. When feeder i and feeder j are linked, $a_{ij} = 1$; otherwise $a_{ij} = 0$

The key to the incidence matrix is the linking relationship between each of the two feeders in a distribution system, which can be identified from the DSSR expressions. The identification process can be summarised in the following two situations.

First, if the variables of power loads at two feeders (e.g. feeder i and feeder j) appear in the same constraint as in Equation (4) or Equation (6), these two feeders are directly linked with each other and the corresponding matrix element $a_{(i,j)}$ is set as 1. This can be illustrated by the example of the first constraint in Equation (7) (i.e. $S_{F,1} + S_{F,2} \le c_{F,2}$) Since the constraint contains the power loads $S_{F,1}$ and $S_{F,2}$, their associated matrix element $a_{(1,2)}$ is set as 1, indicating that feeders F_1 and F_2 are directly linked and the power loads under these feeders should not exceed the capacity of the transferred feeder F_2.

Second, if the variables of power loads at feeder i and feeder j appear in different DSSR constraints, but these constraints are dependent in terms of these two variables, the two feeders are indirectly linked. Under this situation, the matrix element $a_{(i,j)}$ should also be set as 1. This is because if constraints associated with two variables are not independent, a change of one variable will affect the range of the value for the other variable. Therefore, the two variables (or the two feeders) are indirectly linked with each other. Take the fourth and the fifth constraints of (7) (i.e. $S_{F,4} + S_{F,3} \le c_{F,3}$ and $S_{F,5} + S_{F,3} \le c_{F,3}$) as an example. From these constraints, the allowable transferred power loads $S_{F,4}$ and $S_{F,5}$ are both influenced by the power load $S_{F,3}$, which indicates the indirect linking relationship between feeders F4 and F5. Therefore, their associated matrix element is recorded as 1.

Following the generation process of the incidence matrix above, the whole incidence matrix for the case network in Figure 1 is shown in Figure 2 for reference.

3.3 | Block matrix

Step 3: Divide the incidence matrix into block matrices [29]. If a matrix is partitioned by sequential partitions of its rows and columns, the resulting partitioned matrix is called a block matrix.

The obtained incidence matrix in *Step 2* can be further divided into block matrices by identifying non-zero elements following two ways.

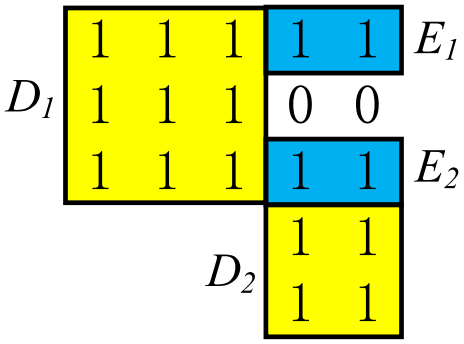

FIGURE 2 The incidence matrix and the results of block matrices of the five-feeder case network.

3-1: Obtain the diagonal block matrices (D_i). For the generation of block matrix D_1, firstly use a_{11} as the first element, then find the largest all-ones square matrix as D_1. The generation of other block matrices follows the similar way. The difference is the first element for D_i ($i \neq 1$) uses the first element of the remaining diagonal elements after generation of D_1-D_{i-1}. The generation of the block matrices stops when a_{nn} is included. Following the generation process of the block matrices, the scale of D_i is $d_i \times d_i$, and the dimension of D_i is d_i.

3-2: Obtain the non-diagonal block matrices (E_i), all with non-zero elements. The scale of E_i is $e_i \times e_j$, and the dimension of E_i is $e_i + e_j$. Due to the symmetry of the incidence matrix, a more efficient way is to obtain the non-diagonal block matrices in the upper-triangular part of the incidence matrix. And the diagonal block matrices in the lower-triangular part is symmetric with those in the upper-triangular part.

The division of the incidence matrix and the results of the block matrices of the case network are shown in Figure 2.

3.4 | DSSR dimension

Step 4: Calculate the DSSR dimension.

As with Section 2.2, the DSSR dimension is defined as the maximum value of the number of feeders with links in this paper. Since one block matrix represents a group of feeder combination (i.e. the combination of feeders linked with each other through the tie switches), the DSSR dimension in Equation (1) is equal to the maximum value of the block matrix dimension as follows:

$$D_m = \max\{d_i, e_i + e_j\} \tag{9}$$

d_i is the number of rows and columns of the diagonal block matrix; e_i and e_j is the number of rows and columns of the non-diagonal block matrix respectively. For the case in Figure 1, at most three feeders (i.e. F1, F2, F3 or F1, F4, F5 or F3, F4, F5) are directly or indirectly linked. Therefore, the dimension of the network is 3, which can be obtained from the diagonal block matrix D_1 with the maximum rows/columns (or the non-diagonal matrix E_1 or E_2 with the maximum sum of rows and columns) in Figure 2.

4 | DECOUPLING AND DIMENSION REDUCTION METHOD OF DSSR

Based on the DSSR dimension calculation method, this section provides the decoupling and dimension reduction method for DSSR. From the obtained block matrices, the distribution network can be decoupled as follows. The remaining steps are as follows.

Step 5: Extract the feeder combinations corresponding to the diagonal block matrix D_i and the non-diagonal block matrix E_i. The feeders associated with the row and column elements of a block matrix can form a group of feeder combinations.

Step 6: Divide the distribution network into several sub-networks according to the feeder combinations. The feeders in each group of feeder combinations can form a sub-network. In this regard, feeders without electrical connections after N-1 fault are decoupled. In other words, a large-scale distribution network can be divided into several smaller-scale sub-networks. Accordingly, the corresponding high-dimensional security region of the network can be divided into several lower-dimensional security regions, which achieves the dimension reduction for the high-dimensional security regions.

5 | CASE STUDY

5.1 | Overview

The 10 kV distribution network case in Figure 3 [24] is used for the case study. This case has 4 substation transformers and 28 feeders. The capacities of transformers and feeders are 80MVA and 10MVA respectively.

The calculations of DSSR are carried out on a 64-bit Window 10 with Intel(R) Core(TM) i5-10200H @ 2.40 GHz CPU, 8 GB RAM.

5.2 | Calculation of DSSR dimension

5.2.1 | DSSR expressions

Step 1: Obtain the expression of DSSR for the case network. The power load should satisfy N-1 security constraints.

The DSSR expression for the 28-feeder case (denoted as $\boldsymbol{\Omega}_{\mathrm{DSSR}}$) is established as below:

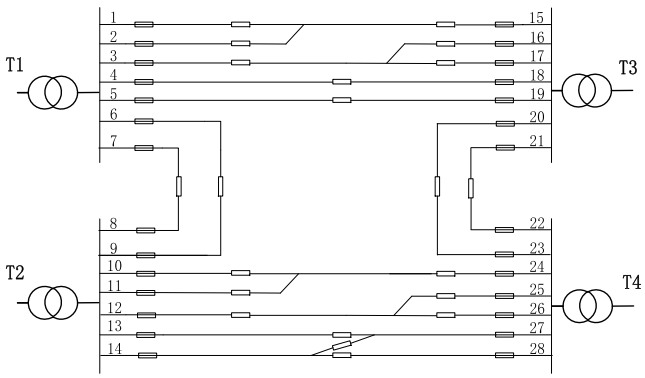

FIGURE 3 28-feeder case.

$$\boldsymbol{\Omega}_{\mathrm{DSSR}}=\left\{W\left|\begin{array}{l}S_{F,4}+S_{F,18}\le\min\left\{c_{F,4},c_{F,18}\right\}\\S_{F,5}+S_{F,19}\le\min\left\{c_{F,5},c_{F,19}\right\}\\S_{F,6}+S_{F,9}\le\min\left\{c_{F,6},c_{F,9}\right\}\\S_{F,7}+S_{F,8}\le\min\left\{c_{F,7},c_{F,8}\right\}\\S_{F,20}+S_{F,23}\le\min\left\{c_{F,20},c_{F,23}\right\}\\S_{F,21}+S_{F,22}\le\min\left\{c_{F,21},c_{F,22}\right\}\\S_{F,13}+S_{F,27}\le\min\left\{c_{F,13},c_{F,27}\right\}\\S_{F,14}+S_{F,27}\le\min\left\{c_{F,14},c_{F,27}\right\}\\S_{F,14}+S_{F,28}\le\min\left\{c_{F,14},c_{F,28}\right\}\\S_{F,1\sim5}+S_{F,15\sim21}\le c_{T,3}\\S_{F,6\sim14}\le c_{T,2}\\S_{F,1\sim9}\le c_{T,1}\\S_{F,10\sim14}+S_{F,22\sim28}\le c_{T,4}\\S_{F,1\sim7}+S_{F,15\sim19}\le c_{T,1}\\S_{F,20\sim28}\le c_{T,4}\\S_{F,15\sim23}\le c_{T,3}\\S_{F,8\sim14}+S_{F,24\sim28}\le c_{T,2}\\\boldsymbol{\Omega}_{\mathrm{DSSR1}}\\\boldsymbol{\Omega}_{\mathrm{DSSR2}}\\\boldsymbol{\Omega}_{\mathrm{DSSR3}}\\\boldsymbol{\Omega}_{\mathrm{DSSR4}}\end{array}\right.\right\}\tag{10}$$

$S_{F,i\sim j}$ means the sum of $S_{F,i}$ to $S_{F,j}$. For instance, $S_{F,1\sim5}$ is $S_{F,1}+S_{F,2}+S_{F,3}+S_{F,4}+S_{F,5}$.

$\boldsymbol{\Omega}_{\mathrm{DSSRx}}$ ($x=1,2,3,4$) are the N-1 security constraints of the four two-supply-one-backup connection modes in the case. For each two-supply-one-backup connection, one feeder is used as a backup for two other feeders. For clarity, $\boldsymbol{\Omega}_{\mathrm{DSSRx}}$ ($x=1,2,3,4$) are written separately as follows:

$$\boldsymbol{\Omega}_{\mathrm{DSSR1}}=\left\{W\left|\begin{array}{l}-\\S_{F,1}+S_{F,15}\le\min\left\{c_{F,1},c_{F,15}\right\}\\S_{F,2}+S_{F,15}\le c_{F,15}\end{array}\right.\right\}\cup$$

$$\left\{W\left|\begin{array}{l}S_{F,1}+S_{F,2}\le\min\left\{c_{F,1},c_{F,2}\right\}\\-\\S_{F,2}+S_{F,15}\le c_{F,2}\end{array}\right.\right\}\cup\tag{11}$$

$$\left\{W\left|\begin{array}{l}S_{F,1}+S_{F,2}\le\min\left\{c_{F,1},c_{F,2}\right\}\\S_{F,1}+S_{F,15}\le c_{F,1}\\-\end{array}\right.\right\}$$

$$\boldsymbol{\Omega}_{\mathrm{DSSR2}}=\left\{W\left|\begin{array}{l}-\\S_{F,3}+S_{F,17}\le\min\left\{c_{F,3},c_{F,17}\right\}\\S_{F,16}+S_{F,17}\le C_{F,17}\end{array}\right.\right\}\cup$$

$$\left\{W\left|\begin{array}{l}S_{F,3}+S_{F,16}\le\min\left\{c_{F,3},c_{F,16}\right\}\\-\\S_{F,16}+S_{F,17}\le c_{F,16}\end{array}\right.\right\}\cup\tag{12}$$

$$\left\{W\left|\begin{array}{l}S_{F,3}+S_{F,16}\le\min\left\{c_{F,3},c_{F,16}\right\}\\S_{F,3}+S_{F,17}\le c_{F,3}\\-\end{array}\right.\right\}$$

$$\boldsymbol{\Omega}_{\mathrm{DSSR3}}=\left\{W\left|\begin{array}{l}-\\S_{F,10}+S_{F,24}\le\min\left\{c_{F,10},c_{F,24}\right\}\\S_{F,11}+S_{F,24}\le C_{F,24}\end{array}\right.\right\}\cup$$

$$\left\{W\left|\begin{array}{l}S_{F,10}+S_{F,11}\le\min\left\{c_{F,10},c_{F,11}\right\}\\-\\S_{F,11}+S_{F,24}\le c_{F,11}\end{array}\right.\right\}\cup\tag{13}$$

$$\left\{W\left|\begin{array}{l}S_{F,10}+S_{F,11}\le\min\left\{c_{F,10},c_{F,11}\right\}\\S_{F,10}+S_{F,24}\le c_{F,10}\\-\end{array}\right.\right\}$$

$$\boldsymbol{\Omega}_{\mathrm{DSSR4}}=\left\{W\left|\begin{array}{l}-\\S_{F,12}+S_{F,26}\le\min\left\{c_{F,12},c_{F,26}\right\}\\S_{F,25}+S_{F,26}\le c_{F,26}\end{array}\right.\right\}\cup$$

$$\left\{W\left|\begin{array}{l}S_{F,12}+S_{F,25}\le\min\left\{c_{F,12},c_{F,25}\right\}\\-\\S_{F,25}+S_{F,26}\le c_{F,25}\end{array}\right.\right\}\cup\tag{14}$$

$$\left\{W\left|\begin{array}{l}S_{F,12}+S_{F,25}\le\min\left\{c_{F,12},c_{F,25}\right\}\\S_{F,12}+S_{F,26}\le c_{F,12}\\-\end{array}\right.\right\}$$

5.2.2 | Incidence matrix

Step 2: Generate the incidence matrix from the DSSR expression. The identification process can be summarised in the following two situations.

First, if the variables of two power loads at two feeders (e.g. feeder i and feeder j) appear in the same constraints as in Equation (10), the corresponding matrix element $a_{(i,j)}$ is set as 1. For example, $S_{F,1\sim5}+S_{F,15\sim21}\le c_{T,3}$, power loads such as $S_{F,1}$, $S_{F,2}$, $S_{F,3}$ are in this formula, then $a_{(1,2)}$, $a_{(1,3)}$ and $a_{(2,3)}$ are recorded as 1.

Second, if the variables of power loads at feeder i and feeder j appear in different DSSR constraints, but these constraints are dependent in terms of these two variables, the matrix element $a_{(i,j)}$ should also be set as 1. For example, $S_{F,13} + S_{F,27} \leq \min\{c_{F,13}, c_{F,27}\}$ and $S_{F,14} + S_{F,27} \leq \min\{c_{F,14}, c_{F,27}\}$, the $a_{(13,14)}$ is recorded as 1.

5.2.3 | Block matrix

Following the step 3 in Section 3.3, the divided results of block matrices are shown in Figure 4.

From Figure 4, the incidence matrix can be divided into four diagonal block matrices (i.e., D_1-D_4 marked in yellow) and six non-diagonal block matrices (i.e. E_1-E_6 marked in blue). D_1-D_4 and E_1-E_6 are numbered from the top-left to the bottom-right.

Following the definition of DSSR dimension in Section 3.4, the dimensions of the block matrices for the 28-feeder case are summarised in Table 1. The scales of these block matrices are also shown for reference.

5.2.4 | DSSR dimension

From Table 1, the DSSR dimension is 12, which corresponds to the largest dimension among the block matrices, that is, the dimension of E_1, E_2 or E_5. Therefore, the time complexity of DSSR calculation algorithms is $O(n^{12})$.

5.3 | Decoupling and dimension reduction of DSSR

5.3.1 | Feeder combination

Corresponding to the diagonal and non-diagonal block matrices in Table 1, 10 feeder combinations are obtained in Table 2.

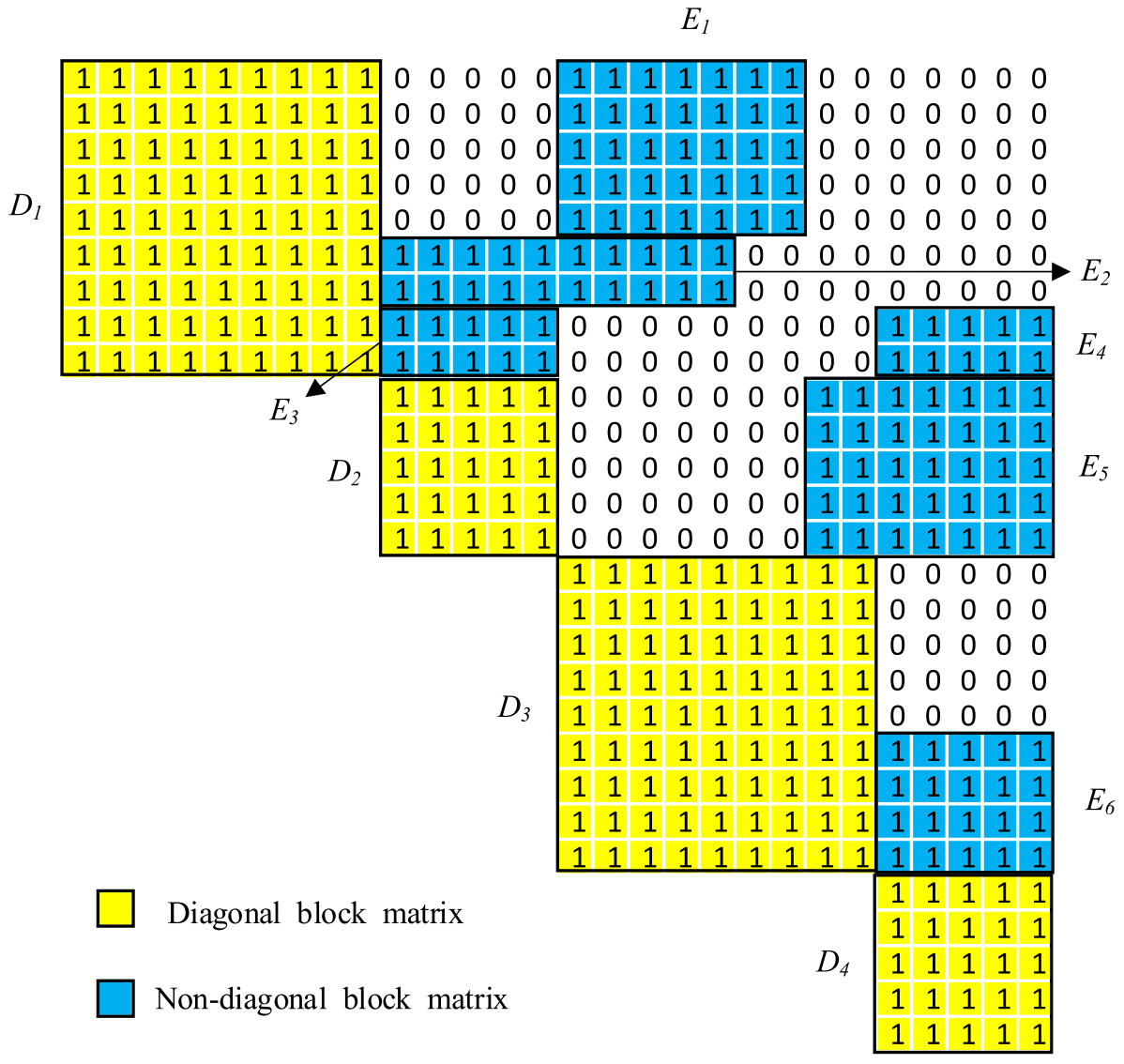

FIGURE 4 Incidence matrix blocking.

TABLE 1 The scale and dimension of block matrices of the 28-feeder case.

Block matrix	Scale	Dimension
D_1	9 × 9	9
D_2	5 × 5	5
D_3	9 × 9	9
D_4	5 × 5	5
E_1	5 × 7	12
E_2	2 × 10	12
E_3	2 × 5	7
E_4	2 × 5	7
E_5	5 × 7	12
E_6	4 × 5	9

TABLE 2 Block matrices and its corresponding feeder combinations.

Block matrix	Feeder combination
D_1	F1-F9
D_2	F10-F14
D_3	F15-F23
D_4	F24-F28
E_1	F1-F5, F15-F21
E_2	F6, F7, F10-F19
E_3	F8-F14
E_4	F8, F9, F24-F28
E_5	F10-F14, F22-F28
E_6	F20-F28

Take E_1 as an example: E_1 contains the elements at the intersection of rows 1-5 and columns 15–21, so the feeders associated with 1-5 rows and 15–21 columns elements can form a group of feeder combination, that is, (F1-F5, F15-F21).

5.3.2 | Decoupling and dimension reduction

The obtained feeder combinations can decouple the distribution network into ten sub-networks with no more than 12 feeders.

The 4 sub-networks obtained from the feeder combinations of diagonal block matrices are shown in Figure 5, while the 6 sub-networks obtained from the feeder combinations of non-diagonal block matrices are shown in Figure 6. Accordingly, the corresponding 28-dimensional security region of the network is divided into 10 lower-dimensional security regions, which achieves the dimension reduction for the high-dimensional security region of the original distribution network.

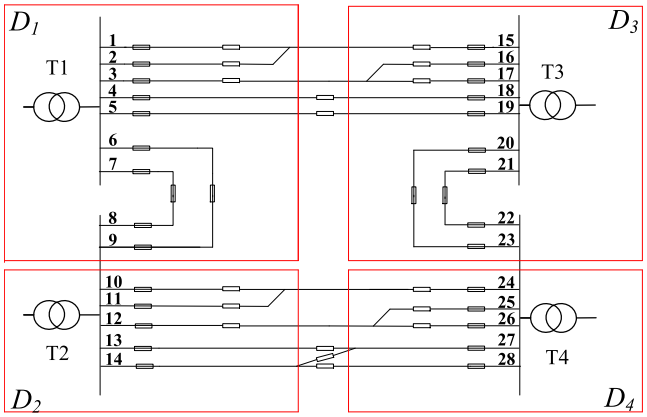

FIGURE 5 Sub-networks obtained from the feeder combinations of diagonal block matrices.

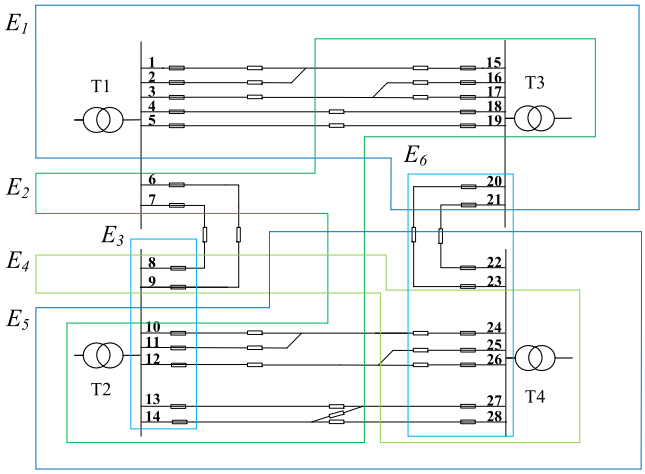

FIGURE 6 Sub-networks obtained from the feeder combinations of non-diagonal block matrices.

5.4 | Application: TSC curve calculation

TSC refers to the maximum load supply capability of a distribution network when it meets the N-1 security criterion [30]. Since the load information is contained in the boundary points of the security region of the distribution network, the TSC can be obtained by summing the loads at the boundary points [15]. The TSC curve can be obtained by arranging the TSC values corresponding to the respective boundary points in order. Compared with TSC, the TSC curve fully describes the extreme load-carrying capability of a distribution network [15].

The proposed decoupling and dimension reduction method in this paper is applied to accelerate the calculation of TSC curve [28], which is a typical DSSR-associated calculation. To verify the effectiveness of the proposed method, the result is compared with that calculated by using the existing algorithm in ref. [28]. It should be mentioned that the algorithm in ref. [28] is also used to calculate the TSC curve after using the proposed method to decouple the case network into multiple sub-networks.

Since the existing algorithm in ref. [28] is based on sampling the state space of security region, this DSSR-associated calculation is very time-consuming when applying to large-scale distribution networks. By using the method proposed in this paper, the dimension of DSSR is reduced from 28 to 12. Therefore, the time complexity of DSSR calculation algorithm is also reduced from $O(n^{28})$ to $O(n^{12})$, which reduces more than 50%.

The sampling step s when sampling the strict boundary is 10MVA. The number of sampling points is denoted as $\left(\frac{10}{s}+1\right)^N$, where $\left(\frac{10}{s}+1\right)$ is the number of points that can be sampled on each boundary and N is the number of feeders [28].

The calculation process and computation time of a 36-feeder case are given in the Appendix A.

The results of TSC curve of the 28-case network before and after using the proposed method in this paper are compared, which are shown in Table 3.

After sampling the strict boundary, TSC curve is plotted by taking the sampling number as abscissa and the total feeder load as ordinate [28]. The TSC curves of sub-networks were calculated; then the TSC curve "summary after decoupling" was obtained, the detailed data and process is in Appendix B. After summary, the TSC curve is exactly the same as that before decoupling, which verifies the effectiveness of the proposed method. The reason why the TSC curve with the use of decoupling is the same as the one without decoupling is as follows:

Firstly, the upper and lower limits of the TSC curve before and after decoupling are the same. There are no overlap feeders in which there are tie switches connected between different sub-networks after decoupling, which ensures independent analysis of the sub-networks. In this regard, the range of the feeder load that satisfy N-1 security constraints stays the same after decoupling. Secondly, since the sampling step is constant, the sampling values of the feeder loads before and after decoupling are the same. These two factors result in the fact that the range of the total load of each boundary point of DSSR (i.e. the TSC value) remains unchanged.

Secondly, the shape of the TSC curve stays the same after the decoupling of the distribution network. The shape of the TSC curve is determined by the proportion of different TSC values on the TSC curve. Since the ranges of different feeder load and the sampling values are unchanged after decoupling, the distribution and proportion of feeder loads in each sub-network are the same as those before decoupling. The summary of TSC curve after decoupling aims at obtaining the Cartesian product of the vectors of the points on the security boundary, and each element of the Cartesian product is composed of the feeder variables selected from each vector of the points on the security boundary in order. Therefore, the distribution and proportion of the feeder loads after summation are the same as those before decoupling. Since the proportions of different TSC values on TSC curve before and after decoupling are the same, the shape of the TSC curve keeps the same.

In summary, the upper and lower limits and the shape of the TSC curve before and after decoupling are the same, hence the TSC curve with the use of decoupling is the same as the one without decoupling.

The computation time and memory are compared in Table 4.

The total time of calculating TSC curve after decoupling is 7.842 ms, which comprises 6.348 ms for the establishment and decoupling of the incidence matrix and 1.494 ms for the TSC curve calculation. The total time for calculating TSC curve using the proposed method in the paper is only approximately 0.05% of the time before decoupling. This shows that the proposed method can significantly accelerate the calculation of TSC curve especially in large-scale distribution networks. With a fixed sampling step, the number of sampling points for calculating the TSC curve grows exponentially with the number of feeder lines. By using the method proposed in this paper to split the incidence matrix of the security region into blocks, the distribution network can be decoupled into multiple sub-networks with fewer feeder lines, thereby significantly

TABLE 3 Total Supply Capability (TSC) curves before and after decoupling.

Network	TSC curve
Before decoupling	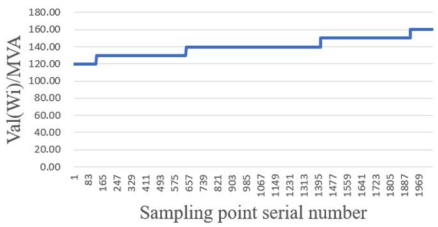
Summary after decoupling	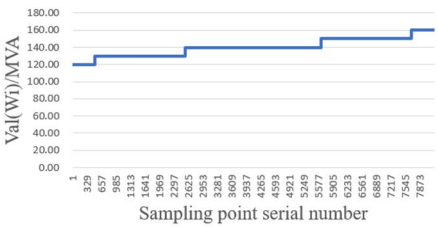

TABLE 4 Computation time and memory before and after decoupling.

Network	Time(ms)	Requested memory(kB)	Number of feeders	Number of curve points
Before	14283.412	56	28	2048
After	1.494	—	28	8192
D_1	0.121	0.0703	9	8
D_2	0.112	0.0098	5	2
D_3	0.138	0.0703	9	8
D_4	0.095	0.0098	5	2
E_1	0.274	0.1875	12	16
E_2	0.126	0.0469	12	4
E_3	0.129	0.0137	7	2
E_4	0.106	0.0137	7	2
E_5	0.277	0.0938	12	8
E_6	0.116	0.0703	9	8

reducing the number of sampling points and improving the performance of TSC curve calculation.

The condition of the acceleration is that the distribution network can be decoupled and the DSSR dimension can be reduced. The only one exception is that the network is fully linked between feeders, which is explained in Appendix C. Since a real distribution network contains many substations, of which the feeders are normally not fully linked as the case in Appendix C. The methodology in this study can be applicable in most cases.

The computation time and memory are compared in Table 4. The memory during the calculation process is mainly used for storage of the vectors of sampling points on the security boundary. (i.e. the feeder load information contained in the points on the TSC curve). Considering we create int8 variable in MATLAB that takes up 1 byte, the memory usage can be expressed as $x^*N \div 1024$(kb), where x represents the number of sampling points on the security boundary and N represents the number of feeders. As an illustration, consider the first row of Table 4, which corresponds to the network prior to decoupling. With 28 feeders, a total of 2048 TSC curve points are obtained, yielding a memory usage of 56(kb).

The maximum requested memory of the sub-networks is 0.1875kB with only approximately 0.33% of the requested memory before decoupling. This shows that the proposed method can significantly reduce the computation memory of TSC curve. The main memory is used for storing the vectors of the sampling points on the security boundary. Since the vectors of the sampling points on the security boundary is constantly needed during the calculation of the TSC curve, the memory cannot be freed during the calculation.

6 | CONCLUSION

For a large-scale distribution system, the application of the security region methodology normally requires large computer memory and high computation time due to the high dimension of DSSR. To overcome this problem, this paper provides a decoupling and dimension reduction method for the practical application of DSSR, which has significant implications for applying security region analysis methods to large-scale distribution networks in practice. The main contributions are as follows:

(1) DSSR dimension is defined as the maximum number of feeders with links, which is more suitable for dimension reduction compared to the existing definition of DSSR dimension. This definition is able to overcome the shortcomings of large computational cost and difficult transformation of incidence matrix and conform to the traditional definition of dimension as well, an integer responding to the number of parameters.
(2) A DSSR dimension calculation method is proposed, which involves formulating the DSSR expressions associated with the target distribution system, extracting the incidence matrix from these expressions, and generating block matrices based on the obtained incidence matrix. From the case study, the method is easy to be implemented.
(3) A decoupling and dimension reduction method for DSSR based on the dimension calculation method is proposed for the first time. By utilising the method, a distribution system can be decoupled into multiple smaller sub-systems with fewer feeders. Accordingly, this lowers the dimension of the distribution system, facilitating more efficient security analysis of the distribution system.

A 28-feeder case and a 36-feeder case were used to verify the effectiveness of the proposed method. For the calculation of TSC curve (which is proved to be time-consuming in previous studies), the decoupling and dimension reduction method performs more efficiently than the previous studies. For the two cases, the time complexity is reduced by more than 50%, increasing the computation speed by more than a thousand times. Other cases also work well but the specific speedup

depends on the specific case. The proposed method is of great significance for applying DSSR-associated calculations to large-scale distribution networks.

The decoupling method can not only be used in DSSR-associated calculation, but also be used to divide the large-scale distribution system into smaller-scale sub-systems, which is worthy of further study in distribution system analysis. In addition, distributed generators, grid-connected energy storage, and other components in smart distribution network will also be considered in the future.

ACKNOWLEDGEMENTS

This work was supported by the National Natural Science Foundation of China (52177105).

CONFLICT OF INTEREST STATEMENT

The authors declare no conflicts of interest.

DATA AVAILABILITY STATEMENT

The data that support the findings of this study are available on request from the corresponding author. The data are not publicly available due to privacy or ethical restrictions.

ORCID

Yuhao Fan https://orcid.org/0000-0002-9077-0601

REFERENCES

1. Hnyilicza, E., Lee, S.T.Y., Schweppe, F.C.: Steady-state security regions: set-theoretic approach. In: Proceedings of the IEEE PICA Conference (1975)
2. Wu, F.F., Tsai, Y.-K., Yu, Y.-X.: Probabilistic steady-state and dynamic security assessment. IEEE Trans. Power Syst. 3(1), 1–9 (1988). https://doi.org/10.1109/59.43173
3. Liu, C.-C.: A new method for the construction of maximal steady-state security regions of power systems. IEEE Power Eng. Rev.(11), 25–26 (1986). https://doi.org/10.1109/MPER.1986.5527464
4. Zhu, J.: Optimal power system steady-state security regions with fuzzy constraints. In: 2002 IEEE Power Engineering Society Winter Meeting. Conference Proceedings (Cat. No.02CH37309), vol. 2, pp. 1095–1099 (2002). https://doi.org/10.1109/PESW.2002.985180
5. Wu, F., Kumagai, S.: Steady-state security regions of power systems. IEEE Trans. Circ. Syst. 29(11), 703–711 (1982). https://doi.org/10.1109/TCS.1982.1085091
6. Xiao, J., et al.: Distribution system security region (DSSR) for smart grid. In: 2012 China International Conference on Electricity Distribution, pp. 1–4 (2012). https://doi.org/10.1109/CICED.2012.6508587
7. Xiao, J., et al.: Model and topological characteristics of power distribution system security region. J. Appl. Math. 2014, 1–13 (2014). https://doi.org/10.1155/2014/327078
8. Xiao, J., et al.: Observation of security region boundary for smart distribution grid. IEEE Trans. Smart Grid 8(4), 1731–1738 (2017). https://doi.org/10.1109/TSG.2015.2505325
9. Zu, G., Xiao, J., Sun, K.: Mathematical base and deduction of security region for distribution systems with DER. IEEE Trans. Smart Grid 10(3), 2892–2903 (2019). https://doi.org/10.1109/TSG.2018.2814584
10. Yang, T., Yu, Y.: Static voltage security region-based coordinated voltage control in smart distribution grids. IEEE Trans. Smart Grid 9(6), 5494–5502 (2018). https://doi.org/10.1109/TSG.2017.2680436
11. Wan, C., et al.: Maximum uncertainty boundary of volatile distributed generation in active distribution network. IEEE Trans. Smart Grid 9(4), 2930–2942 (2018). https://doi.org/10.1109/TSG.2016.2623760
12. Wang, T., Zhang, S., Gu, X.: A trend-based approach for situation awareness in power systems. Int. Trans. Elect. Energy Syst. 27(12) (2017). https://doi.org/10.1002/etep.2446
13. Xiao, J., Zhang, B., Luo, F.: Distribution network security situation awareness method based on security distance. IEEE Access 7, 37855–37864 (2019). https://doi.org/10.1109/ACCESS.2019.2906779
14. Liu, J., et al.: Stochastic multi-objective distribution feeder reconfiguration based on point estimation considering N-1 security and net loss. In: 2016 IEEE Power and Energy Society General Meeting (PESGM) (2016). https://doi.org/10.1109/pesgm.2016.7741616
15. Xiao, J., et al.: Boundary supply capability for distribution systems: concept, indices and calculation. IET Gener. Transm. Distrib. 12(2), 499–506 (2017). https://doi.org/10.1049/iet-gtd.2017.0725
16. Xiao, J., et al.: Security distance for distribution system: definition, calculation, and application. Int. Trans. Elect. Energy Syst. 29(5), e2838 (2019). https://doi.org/10.1002/2050-7038.2838
17. Chen, S., et al.: Steady-state security regions of electricity-gas integrated energy systems. In: 2016 IEEE Power and Energy Society General Meeting (PESGM), pp. 1–5 (2016). https://doi.org/10.1109/PESGM.2016.7741474
18. Clegg, S., Mancarella, P.: Integrated modeling and assessment of the operational impact of power-to-gas (P2G) on electrical and gas transmission networks. IEEE Trans. Sustain. Energy 6(4), 1234–1244 (2015). https://doi.org/10.1109/TSTE.2015.2424885
19. Liu, Y., et al.: Quantitatively estimating and evaluating macroscopic scale of power transmission and distribution network. In: 2006 International Conference on Power System Technology, pp. 1–5 (2006). https://doi.org/10.1109/ICPST.2006.321465
20. Long, W., et al.: Evaluation indicators and methods on the sufficiency level of the scale of networks. Electrotech. Appl. 35(05), 20–23 (2015). (in Chinese)
21. Li, X., et al.: Indices system and its application for evaluating planning scale of HV distribution network. Proc. CSEE 17, 18–27 (2006). (in Chinese). https://doi.org/10.3321/j.issn:0258-8013.2006.17.004
22. Engelking, R.: Definition of the small inductive dimension. In: Dimension Theory, 1st 1st ed, pp. 3–10. Netherland (1978)
23. Roman, S.: Vector spaces. In: Advanced Linear Algebra, 2nd ed, pp. 33–54. USA (1995). ch. 1
24. Xiao, J., Su, Y., Zhang, H.: Dimension of distribution system security region: concept, calculation and application. IET Gener. Transm. Distrib. 14(12), 16–22 (2020). https://doi.org/10.1049/iet-gtd.2019.0999
25. Yang, T., Yu, Y.: Steady-state security region-based voltage/var optimization considering power injection uncertainties in distribution grids. IEEE Trans. Smart Grid 10(3), 2904–2911 (2018). https://doi.org/10.1109/tsg.2018.2814585
26. Jiang, X., et al.: Feasible operation region of an electricity distribution network. Appl. Energy 331, 120419 (2023). https://doi.org/10.1016/j.apenergy.2022.120419
27. Frakes, W., Baeza-Yates, R.: Analysis in Information Retrieval: Data Structures and Algorithms, pp. 379–384. Prentice-Hall, Inc. (1992). ch. 12, sec7
28. Xiao, J., et al.: Mathematical model and mechanism of TSC curve for distribution networks. Int. J. Electr. Power Energy Syst. 137(Jan), 107812 (2022). https://doi.org/10.1016/J.IJEPES.2021.107812
29. Horn, R.A., Johnson, C.R.: Partitioned sets and matrices. In: Matrix Analysis, 2nd ed, pp. 16–21 (2012). Cambridge University Press
30. Xiao, J., et al.: Total supply capability and its extended indices for distribution systems: definition, model, calculation and applications IET Generation. Transm. Distrib. 5(8), 869–876 (2011). https://doi.org/10.1049/iet-gtd.2010.0769

How to cite this article: Xiao, J., Fan, Y., Jiang, X.: Decoupling and dimension reduction method for distribution system security region. IET Energy Syst. Integr. 1–17 (2023). https://doi.org/10.1049/esi2.12105

APPENDIX A

Decoupling and dimension reduction calculation for TSC curve of 36-feeder case

For the 36-feeder case, in the computation environment described in 5.1 of this paper, the TSC curve cannot be calculated due to the lack of memory by using the method in ref. [28]. After using the proposed method, the time for TSC curve calculation is 4.946 ms and the maximum requested memory is 1kB.

The computation process is given below.

A.1 | Overview

This case in Figure A1 has 4 substation transformers and 36 feeders. The detailed capacities of the transformers and feeders can refer to Section 5.1.

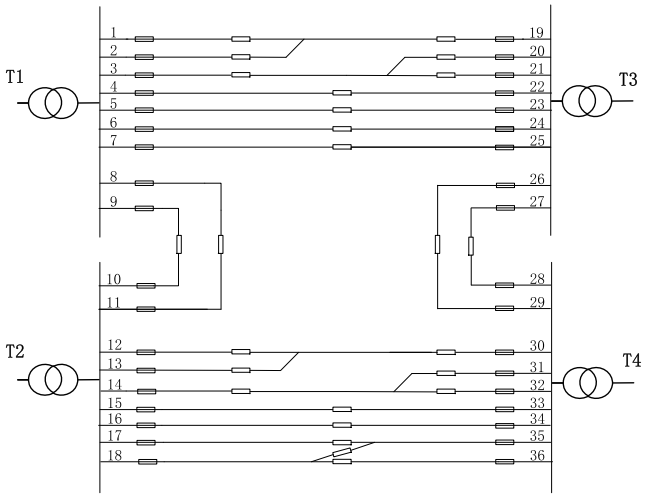

FIGURE A1 36-feeder case.

A.2 | DSSR expressions

$$\boldsymbol{\Omega}_{\mathrm{DSSR}}=\left\{W\left|\begin{array}{l}S_{F,4}+S_{F,22}\le\min\{c_{F,4},c_{F,22}\}\\S_{F,5}+S_{F,23}\le\min\{c_{F,5},c_{F,23}\}\\S_{F,6}+S_{F,24}\le\min\{c_{F,6},c_{F,24}\}\\S_{F,7}+S_{F,25}\le\min\{c_{F,7},c_{F,25}\}\\S_{F,8}+S_{F,11}\le\min\{c_{F,8},c_{F,11}\}\\S_{F,9}+S_{F,10}\le\min\{c_{F,9},c_{F,10}\}\\S_{F,26}+S_{F,29}\le\min\{c_{F,26},c_{F,29}\}\\S_{F,27}+S_{F,28}\le\min\{c_{F,27},c_{F,28}\}\\S_{F,15}+S_{F,33}\le\min\{c_{F,15},c_{F,33}\}\\S_{F,16}+S_{F,34}\le\min\{c_{F,16},c_{F,34}\}\\S_{F,17}+S_{F,35}\le\min\{c_{F,17},c_{F,35}\}\\S_{F,35}+S_{F,18}\le\min\{c_{F,18},c_{F,35}\}\\S_{F,18}+S_{F,36}\le\min\{c_{F,18},c_{F,36}\}\\S_{F,1\sim7}+S_{F,19\sim27}\le c_{T,3}\\S_{F,8\sim18}\le c_{T,2}\\S_{F,1\sim9}+S_{F,19\sim25}\le c_{T,1}\\S_{F,26\sim36}\le c_{T,4}\\S_{F,1\sim11}\le c_{T,1}\\S_{F,12\sim18}+S_{F,28\sim36}\le c_{T,4}\\S_{F,19\sim29}\le c_{T,3}\\S_{F,10\sim18}+S_{F,30\sim36}\le c_{T,2}\\\boldsymbol{\Omega}_{\mathrm{DSSR5}}\\\boldsymbol{\Omega}_{\mathrm{DSSR6}}\\\boldsymbol{\Omega}_{\mathrm{DSSR7}}\\\boldsymbol{\Omega}_{\mathrm{DSSR8}}\end{array}\right.\right\}\tag{A1}$$

$\boldsymbol{\Omega}_{\mathrm{DSSRx}}$ ($x=5,6,7,8$) are written separately as follows:

$$\boldsymbol{\Omega}_{\mathrm{DSSR5}}=\left\{W\left|\begin{array}{l}-\\S_{F,1}+S_{F,19}\le\min\{c_{F,1},c_{F,19}\}\\S_{F,2}+S_{F,19}\le c_{F,19}\end{array}\right.\right\}\cup$$
$$\left\{W\left|\begin{array}{l}S_{F,1}+S_{F,2}\le\min\{c_{F,1},c_{F,2}\}\\-\\S_{F,2}+S_{F,19}\le c_{F,2}\end{array}\right.\right\}\cup\tag{A2}$$
$$\left\{W\left|\begin{array}{l}S_{F,1}+S_{F,2}\le\min\{c_{F,1},c_{F,2}\}\\S_{F,1}+S_{F,19}\le c_{F,1}\\-\end{array}\right.\right\}$$

$$\boldsymbol{\Omega}_{\mathrm{DSSR6}}=\left\{W\left|\begin{array}{l}-\\S_{F,3}+S_{F,21}\le\min\{c_{F,3},c_{F,21}\}\\S_{F,20}+S_{F,21}\le c_{F,21}\end{array}\right.\right\}\cup$$
$$\left\{W\left|\begin{array}{l}S_{F,3}+S_{F,20}\le\min\{c_{F,3},c_{F,20}\}\\-\\S_{F,20}+S_{F,21}\le c_{F,20}\end{array}\right.\right\}\cup\tag{A3}$$
$$\left\{W\left|\begin{array}{l}S_{F,3}+S_{F,20}\le\min\{c_{F,3},c_{F,20}\}\\S_{F,3}+S_{F,21}\le c_{F,3}\\-\end{array}\right.\right\}$$

$$\boldsymbol{\Omega}_{\mathrm{DSSR7}}=\left\{W\left|\begin{array}{l}-\\S_{F,12}+S_{F,30}\le\min\{c_{F,12},c_{F,30}\}\\S_{F,13}+S_{F,30}\le c_{F,30}\end{array}\right.\right\}\cup$$
$$\left\{W\left|\begin{array}{l}S_{F,12}+S_{F,13}\le\min\{c_{F,12},c_{F,13}\}\\-\\S_{F,13}+S_{F,30}\le c_{F,13}\end{array}\right.\right\}\cup\tag{A4}$$
$$\left\{W\left|\begin{array}{l}S_{F,12}+S_{F,13}\le\min\{c_{F,12},c_{F,13}\}\\S_{F,12}+S_{F,30}\le c_{F,12}\\-\end{array}\right.\right\}$$

$$\boldsymbol{\Omega}_{\mathrm{DSSR8}}=\left\{W\left|\begin{array}{l}-\\ S_{F,14}+S_{F,32}\le\min\left\{c_{F,14},c_{F,32}\right\}\\ S_{F,31}+S_{F,32}\le c_{F,32}\end{array}\right.\right\}\cup\left\{W\left|\begin{array}{l}S_{F,14}+S_{F,31}\le\min\left\{c_{F,14},c_{F,31}\right\}\\ -\\ S_{F,31}+S_{F,32}\le c_{F,31}\end{array}\right.\right\}\cup\left\{W\left|\begin{array}{l}S_{F,14}+S_{F,31}\le\min\left\{c_{F,14},c_{F,31}\right\}\\ S_{F,14}+S_{F,32}\le c_{F,14}\\ -\end{array}\right.\right\}\tag{A5}$$

A.3 | Incidence matrix blocking

The divided results of block matrices are shown in Figure A2.

A.4 | Feeder combination

The feeder combinations are obtained in Table A1.

TABLE A1 Block matrices and its corresponding feeder combinations.

Block matrix	Feeder combination
D_1	F1-F11
D_2	F12-F18
D_3	F18-F28
D_4	F30-F36
E_1	F1-F7, F19-F27
E_2	F8, F9, F12-F25
E_3	F10, F11, F12-F18
E_4	F10, F11, F30-F36
E_5	F12-F18, F28-F36
E_6	F26-F36

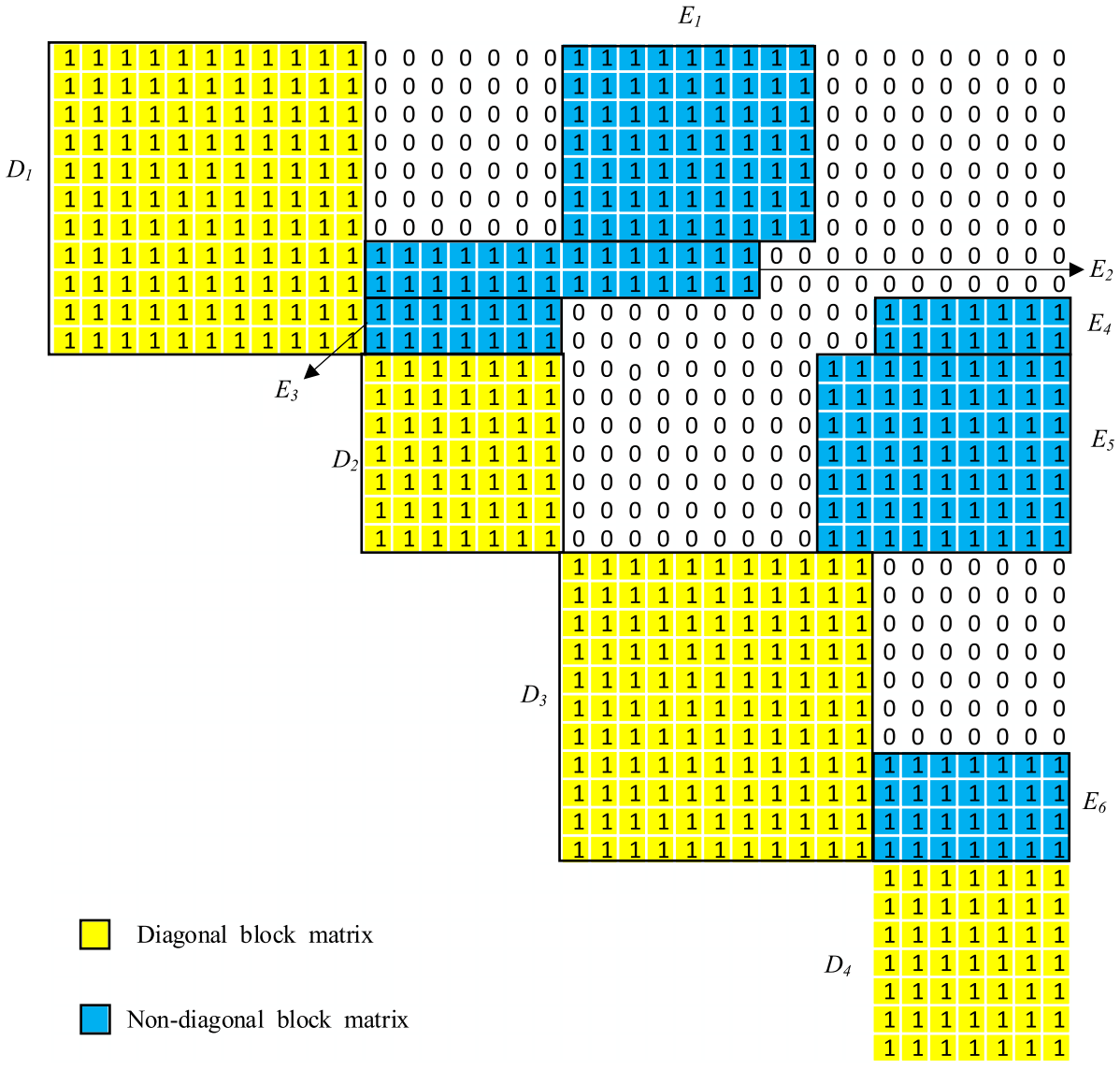

FIGURE A2 Incidence matrix blocking.

A.5 | Decoupling and dimension reduction

The 4 sub-networks obtained from the diagonal block matrices are shown in Figure A3.

The six sub-networks obtained from the non-diagonal block matrices are shown in Figure A4.

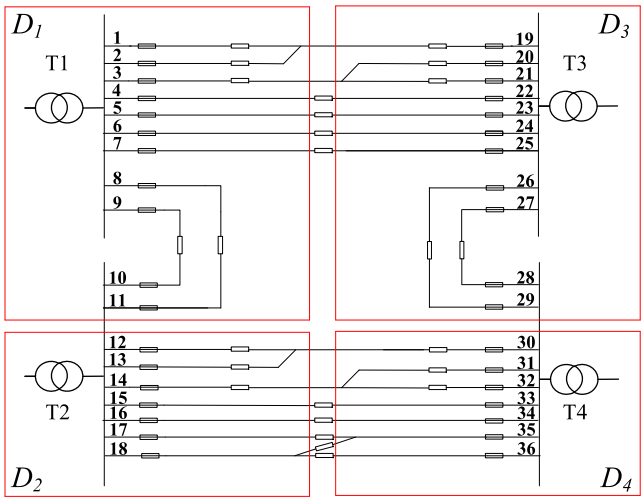

FIGURE A3 Sub-networks obtained from diagonal block matrices.

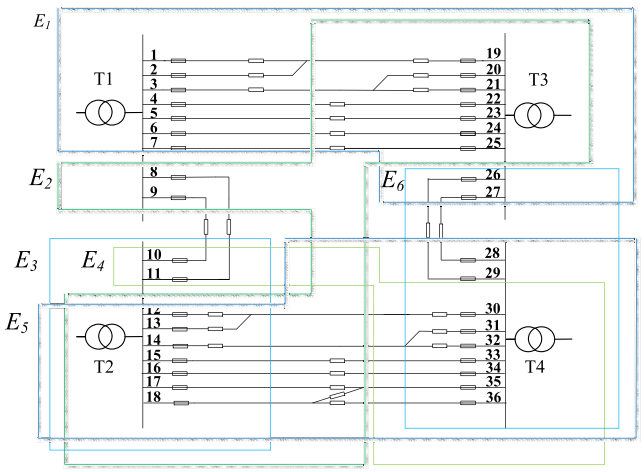

FIGURE A4 Sub-networks obtained from non-diagonal block matrices.

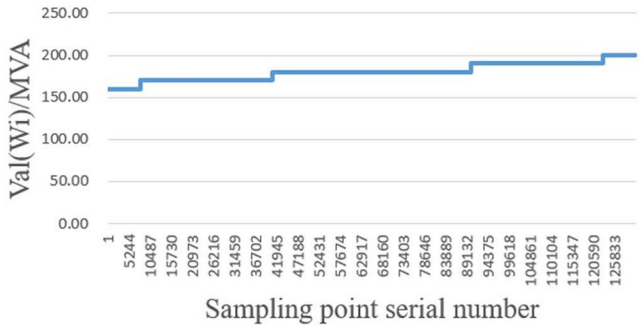

FIGURE A5 Total Supply Capability (TSC) curve of 36-feeder case.

A.6 | TSC curve

The TSC curve points of each sub-network after decoupling are summarised to obtain the TSC curve results of the whole distribution network, as shown in Figure A5.

The computation time is shown in Table A2.

APPENDIX B

Process to obtain the "summary after decoupling" TSC curve of 28-feeder case

The TSC curves of the sub-networks after decoupling are shown in Table B1, which are obtained by the method in [28].

The sub-networks whose TSC curves are not horizontally straight, E_1 and E_5, are treated first. Considering the feeders in which there are tie switches connected, E_1 contains feeders F1-F5 and F15-F19. The distribution of the supply capability of (F1-F5, F15-F19) obtained by the method in [28] is shown in Table B2.

E_5 contains feeders F10-F14 and F24-F28. The distribution of the supply capability of (F10-F14, F24-F28) obtained by the method in ref. [28] is shown in Table B3.

Summarising Table B2 with Table B3, the results are shown in Table B4.

Arrange Table B4 in the order of supply capability from smallest to largest. The results are shown in Table B5.

The whole distribution network has a total of 28 feeders (F1-F28), and some feeders are still missing in Table B5. Then look for the missing feeders from other sub-networks.

D_1 contains feeders F6-F9. The distribution of the supply capability of (F6-F9) obtained by the method in [28] is shown in Table B6.

Summarising Table B5 with Table B6, the results are shown in Table B7.

D_3 contains feeders F20-F23. The distribution of the supply capability of (F20-F23) obtained by the method in [28] is shown in Table B8.

Summarising Table B7 with Table B8, the results are shown in Table B9.

TABLE A2 Decoupling and dimension reduction to calculate Total Supply Capability (TSC) curve time.

Sub-network D_i/E_i	Computation time(ms)	Number of feeders
All networks	4.946	36
D_1	0.112	11
D_2	0.089	7
D_3	0.106	11
D_4	0.091	7
E_1	2.634	16
E_2	0.130	16
E_3	0.096	9
E_4	0.093	9
E_5	1.492	16
E_6	0.103	11

TABLE B1 TSC curves of the sub-networks after decoupling.

Sub-networks	TSC curve
D_1	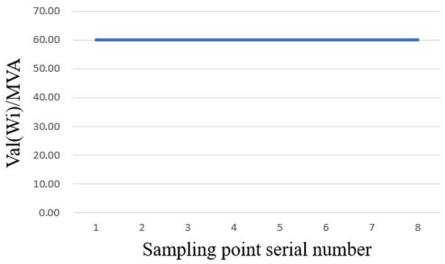
D_2	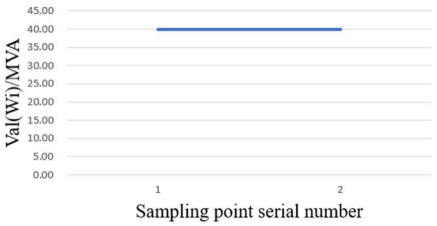
D_3	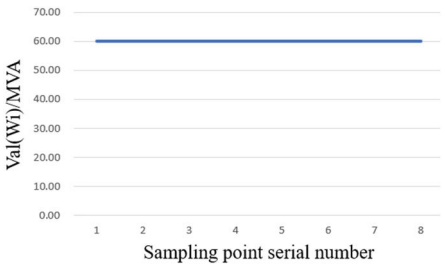
D_4	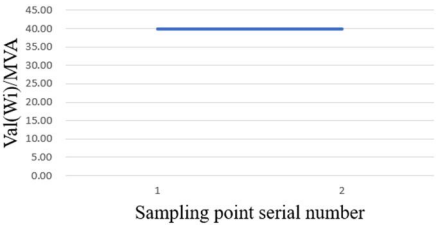
E_1	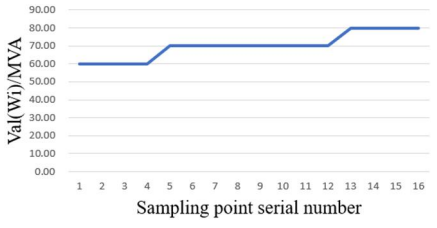
E_2	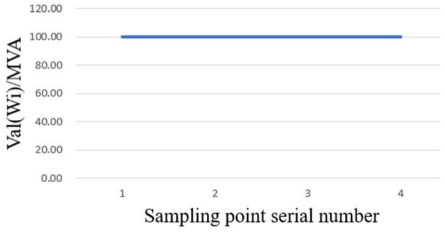

TABLE B1 (Continued)

Sub-networks	TSC curve
E_3	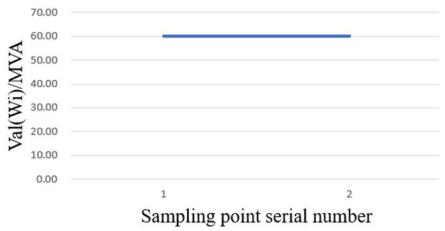
E_4	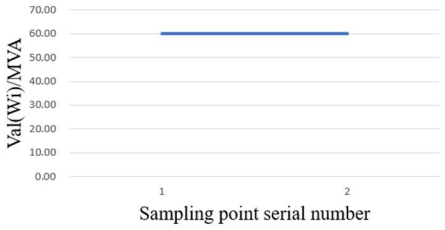
E_5	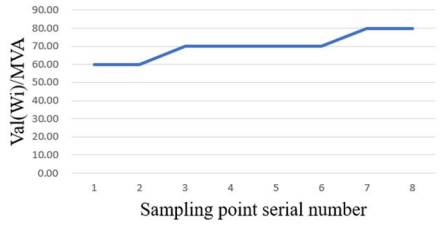
E_6	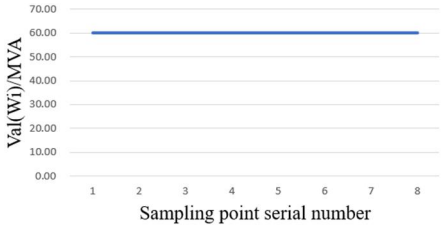

TABLE B2 Sequential distribution of the supply capability of (F1-F5, F15-F19).

Serial number	Supply capability/MVA	Amount
1–4	40	4
5–12	50	8
13–16	60	4

TABLE B3 Sequential distribution of the supply capability of (F10-F14, F24-F28).

Serial number	Supply capability/MVA	Amount
1–2	40	2
3–6	50	4
7–8	60	2

TABLE B4 Distribution of the supply capability of (F1-F5, F10-F19, F24-F28).

Supply capability/MVA	Amount
40 + 40 = 80	4 × 2 = 8
40 + 50 = 90	4 × 4 = 16
40 + 60 = 100	4 × 2 = 8
50 + 40 = 90	8 × 2 = 16
50 + 50 = 100	8 × 4 = 32
50 + 60 = 110	8 × 2 = 16
60 + 40 = 100	4 × 2 = 8
60 + 50 = 110	4 × 4 = 16
60 + 60 = 120	4 × 2 = 8

TABLE B5 Sequential distribution of the supply capability of (F1-F5, F10-F19, F24-F28).

Serial number	Supply capability/MVA	Amount
1–8	80	8
9–40	90	32
41–88	100	48
89–120	110	32
121–128	120	8

TABLE B6 Sequential distribution of the supply capability of (F6-F9).

Serial number	Supply capability/MVA	Amount
1–8	20	8

TABLE B7 Sequential distribution of the supply capability of (F1-F19, F24-F28).

Serial number	Supply capability/MVA	Amount
1–64	80 + 20 = 100	8 × 8 = 64
65–320	90 + 20 = 110	32 × 8 = 256
321–704	100 + 20 = 120	48 × 8 = 384
705–960	110 + 20 = 130	32 × 8 = 256
961–1024	120 + 20 = 140	8 × 8 = 64

TABLE B8 Sequential distribution of the supply capability of (F20-F23).

Serial number	Supply capability/MVA	Amount
1–8	20	8

TABLE B9 Sequential distribution of the supply capability of (F1-F28).

Serial number	Supply capability/MVA	Amount
1–512	100 + 20 = 120	64 × 8 = 512
513–2560	110 + 20 = 130	256 × 8 = 2048
2561–5632	120 + 20 = 140	384 × 8 = 3072
5633–7680	130 + 20 = 150	256 × 8 = 2048
7681–8192	140 + 20 = 160	64 × 8 = 512

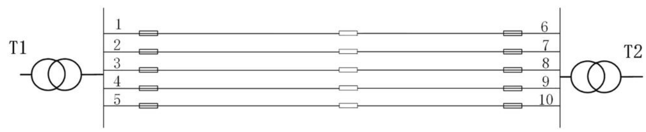

FIGURE C1 10-feeder full-link case.

1	1	1	1	1	1	1	1	1	1
1	1	1	1	1	1	1	1	1	1
1	1	1	1	1	1	1	1	1	1
1	1	1	1	1	1	1	1	1	1
1	1	1	1	1	1	1	1	1	1
1	1	1	1	1	1	1	1	1	1
1	1	1	1	1	1	1	1	1	1
1	1	1	1	1	1	1	1	1	1
1	1	1	1	1	1	1	1	1	1
1	1	1	1	1	1	1	1	1	1

FIGURE C2 Incidence matrix.

This is the end. Table B9 has contained all 28 feeders. Using the first 2 columns of Table B9, the TSC curve can be obtained by a plot software (Microsoft Office Excel used in this paper).

APPENDIX C

Full-link case network that cannot be decoupled

This full-link case network in Figure C1 has 2 substation transformers and 10 feeders.

The corresponding DSSR expression is shown in formula C1.

$$\boldsymbol{\Omega}_{\mathrm{DSSR}} = \left\{ W \left| \begin{array}{l} S_{F,1} + S_{F,6} \le \min\{c_{F,1}, c_{F,6}\} \\ S_{F,2} + S_{F,7} \le \min\{c_{F,2}, c_{F,7}\} \\ S_{F,3} + S_{F,8} \le \min\{c_{F,3}, c_{F,8}\} \\ S_{F,4} + S_{F,9} \le \min\{c_{F,4}, c_{F,9}\} \\ S_{F,5} + S_{F,10} \le \min\{c_{F,5}, c_{F,10}\} \\ \sum_{i=1}^{10} S_{F,i} \le \min\{c_{T,1}, c_{T,2}\} \end{array} \right. \right\} \tag{C1}$$

The corresponding incidence matrix is shown in Figure C2.

The incidence matrix of the full-link case is an all-one matrix, which contains only one block matrix, that is, the incidence matrix itself. Therefore, the full-link case network cannot be decoupled.

For real distribution networks with many substations, they are normally not fully linked and can be decoupled even if the structure of each substation is the same as in Figure C1. For example, the two substations in Figure C3 follow the same structure as in Figure C1, but there are no links between some feeders (e.g. no link between F1 and F20). Therefore, the case in Figure C3 can be decoupled.

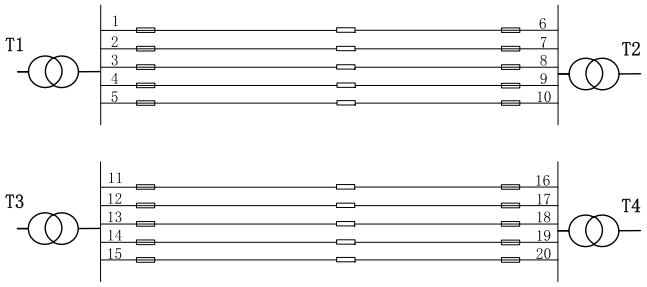

FIGURE C3 The case after replication of substations in Figure C1.